

Color-based underwater object recognition using water light attenuation

Abstract—In this article we present a new approach for object recognition in a robotic underwater context. Color is an attractive feature because of its simplicity and its robustness to scale changes, object positions and partial occlusions. Unfortunately, in the underwater medium, the colors are modified by attenuation and are not constant with the distance. To perform a color-based recognition of an object, we develop an algorithm robust with respect to the attenuation which takes into account the light modification during its path between the light source and the camera. Therefore, a given underwater object can be identified in an image by detecting all the colors compatible with its prior known color. Our method is fast, robust and needs a very few computers resources. We successfully used it when experimenting in the sea using a system we built. It is suitable for robotic applications where computers resources are limited and shared between various embedded devices. This novel concept enables the use of the color in many applications such as target interception, object tracking or obstacle detection.

Index Terms—Vision, color, light attenuation, underwater robot.

I. INTRODUCTION

WITH the development of autonomous underwater vehicles (AUV), the identification of underwater objects remains a major issue [7][15][27].

Usually, in the water, sonar is used for the detection and the classification of objects at long range [16][19]. Vision sensors are then used in the final stage for short range identification. Recently, a number of underwater vehicles have used vision system as main sensing mechanism [5][20] because of their high resolution and low cost.

Unfortunately, in seawater, the light's specific features such as absorption and scattering phenomena, make the vision task more difficult. Underwater imaging suffers from short range, low contrast, non-uniform illumination, diminished colors, and often from prominent green or blue hues [10][18]. Therefore, the literature related to underwater object identification usually shows algorithms based on shape [29][15]. Color is less frequently used as a feature for underwater operations compared to terrestrial ones because of this color constancy problem. The state of the art in underwater color recognition is poor but some works exist in related fields. For example, some algorithms have been developed to process or restore colors [14][21][4][22][28], but as far as we know identification methods do not use the color as a self-sufficient feature.

However, color remains a simple and robust piece of information for underwater object identification [8], even sometimes the most reliable, because the identification based on edge detection is also very limited by underwater vision problems. To deal with color problems, some authors have also tried to embed suitable illumination systems [26] or to estimate with accuracy object surface reflectance spectra [23]. Those

solutions work well but this kind of additional material or additional prior knowledge is a problematic constraint on light autonomous robots. In the specific context of underwater man-made object identification by robots, we often have some very basic knowledge on the object that we are looking for. Shapes and colors are the most common knowledge. It appears essential to find a new method suitable for the underwater environment that is robust to the color constancy problem.

Contribution: Our method is based on the modeling of the color modification by the water. It is a color matching method that enables the use of the color as a single feature to identify objects. It differs with existing methods in the fact that we just work in the RGB space with the raw data coming from the camera. We have focused on the robustness to distance attenuation and to lighting changes. Our method does not need any special material (it has been tested without embedded illumination using webcams in real robot navigation conditions) and requires limited computers resources. Consequently, it can be useful in many robotic applications such as target identification, object tracking, or obstacle detection. A fast calibration is necessary to roughly estimate the underwater medium. Then, a single picture of the object is all that is needed to detect and recognize it.

Contents: In Section II we discuss some background knowledge about the color perception of objects particularly the lighting and the reflection processes. The third section describes the developed color modification model. A discussion on underwater light propagation also appears in this section. Sections IV and V give the object recognition method and the some experimental results. Finally, we conclude in Section VI by discussing future directions for this work.

II. THE COLOR OF AN OBJECT

A. Perception of the object's color

The color perception of an object depends on physical, physiological and psychological components. In this paper, we consider the physical components because the latter two are properties of the visual system of the observer and cannot be integrated in our automatic computer vision process.

There are three physical components:

- the first one is the spectral composition of the light which illuminates the colored object. A light source can be characterized by its spectral distribution¹. The spectrum of light reaching the object determines the reflected color. As a consequence, the same object will appear with different colors whether the sun, an incandescent lamp, or a spot of green light illuminates it.

¹the energy emitted by interval of wavelength.

- the second is the spectral reflectance of the object². Actually, the perception of color depends on the characteristics of the object itself, in particular, the properties of its surface (we consider Lambertian surfaces³). Each object absorbs, transmits, and reflects incident radiation with varying degrees depending on its composition. Color is produced by the absorption of selected wavelengths of light. The object absorbs all other colors except its own colors, which are reflected. For example, a perfectly white object does not absorb any visible radiation.
- the third component is the transmission of light in the medium (e.g. air or water).

B. The object lighting

When an object is lit, it absorbs a part of the light and reflects the rest. Reflection depends on different parameters such as:

- the position and the direction of the light source,
- the color and the intensity of the light source,
- the position and the direction of the object,
- the absorption properties of the object,
- the position and the direction of the observer.

In fact, two kinds of reflections must be taken into account within these parameters: diffuse reflection and specular reflection. To simplify the problem we will assume a rough object with a Lambertian surface in sight, and we will only consider the diffuse reflection.

C. The Lambert reflection model

When a light ray meets an object, a part of the radiation is scattered. Its color and its intensity depends on the absorption properties of the object and on the angle between the incident ray and the surface normal.

The reflected intensity is given by the Lambert Law:

$$I_r = \frac{\rho}{\pi} \cdot \cos(\theta) \cdot I_i, \quad (1)$$

where I_i is the intensity of incident light, ρ is the albedo that is to say the reflecting power of the object's surface (varying between 0 and 1) and θ is the angle between the incident ray and the surface normal.

III. COMPATIBLE COLORS IN AN UNDERWATER ENVIRONMENT

A. Underwater light propagation

Light is a form of electromagnetic radiation which travels at a speed close to $2.2 \times 10^8 \text{ m s}^{-1}$ in the water. When light propagates in water, its intensity decreases exponentially with the distance from the source [6][10][17]. The exponential loss of intensity is called attenuation and has two main origins:

- absorption which is the conversion of electromagnetic energy into other forms of energy, usually heat or chemical energy. The absorbers of the seawater are:

- algae (phytoplankton),
- inorganic and organic particulate matter in suspension (other than algae),
- dissolved organic compounds,
- water itself.
- scattering which simply changes the direction of the electromagnetic energy, as a result of multiple reflections from suspended particles. Scattering by all but the very smallest particles is generally forwards at low angles (we do not consider the back scattered part).

Obviously, the greater the amount of suspended matter, the higher the degree of absorption and scattering. Electromagnetic radiation is characterized by its wavelength and its intensity. Scattering of light by particles is largely independent of wavelength, but not absorption.

B. The Beer-Lambert law

The Beer-Lambert law is an empirical relationship that relates the absorption of light to the properties of the material through which light travels. It describes the exponential decrease of irradiance⁴ with distance, as photons are absorbed and scattered by water and particles. Literature on its theoretical definition and on its purpose can be found in [24][9] and [2][13] respectively. The law is given by:

$$I_{\lambda,d} = I_{\lambda,0} \cdot e^{-c_{\lambda} \cdot d}, \quad (2)$$

where λ is the wavelength, $I_{\lambda,d}$ is the observed intensity of light of wavelength λ at the distance d from the light source, $I_{\lambda,0}$ is the intensity at the light source, c_{λ} is the beam attenuation coefficient for a wavelength λ .

In the oceanographic community, c is universally used for the beam attenuation coefficient also called total attenuation. As we describe the diminution of light intensity for the illuminating light path, assuming a wide beam light source, the diffuse attenuation coefficient may be more appropriate. We will show in the next part how we are able to estimate those parameters.

C. A compatible color surface in RGB space

As discussed previously, the incident light ray is modified during its travel between the light source and the object and then again between the object and the camera (Fig. 1). This modification can be modeled by the following equation:

$$\begin{pmatrix} I_{R,x} \\ I_{G,x} \\ I_{B,x} \end{pmatrix} = \begin{pmatrix} e^{-c_R \cdot d_2} \cdot \frac{\rho}{\pi} \cdot \cos(\theta) \cdot a_R \cdot e^{-c_R \cdot d_1} \\ e^{-c_G \cdot d_2} \cdot \frac{\rho}{\pi} \cdot \cos(\theta) \cdot a_G \cdot e^{-c_G \cdot d_1} \\ e^{-c_B \cdot d_2} \cdot \frac{\rho}{\pi} \cdot \cos(\theta) \cdot a_B \cdot e^{-c_B \cdot d_1} \end{pmatrix} \cdot \begin{pmatrix} I_{R,0} \\ I_{G,0} \\ I_{B,0} \end{pmatrix}$$

where d_1 is the distance between the light source and the object and d_2 the distance between the object and the camera. In a vector form, the irradiance values that the sensor records for the broad range of wavelength λ can be given by:

$$I_{\lambda,x} = \ell \cdot a_{\lambda} \cdot e^{-c_{\lambda} \cdot d}, \quad (3)$$

$$\text{with } \ell = I_{\lambda,0} \cdot \frac{\rho}{\pi} \cdot \cos(\theta), \quad (4)$$

²the fraction of radiant energy that is reflected from its surface.

³for Lambertian surface, the surface luminance is isotropic e.g., light falling on it is scattered such that the apparent brightness of the surface to an observer is the same regardless of the observer's angle of view.

⁴Irradiance is a radiometry term for the power of electromagnetic radiation at a surface, per unit area.

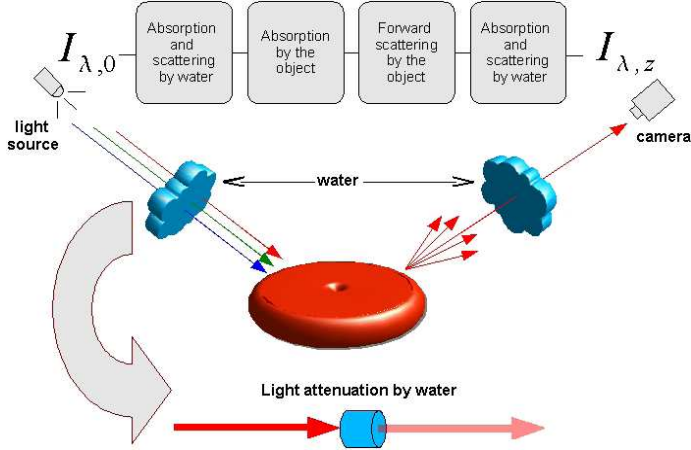


Fig. 1. Model of color modification in an underwater environment.

where ℓ defines the “light” as a parameter related to the modification of the light source intensity and the position of the object, a_λ is the absorption coefficients of the object and d the distance ($d_1 + d_2$).

Definition 1 (Compatible colors): From an underwater point of view, if we consider a colored object lit by a light (natural or artificial), we define as compatible colors all the colors perceived at different distances or at different lighting values. This underwater color definition differs with classical hue value from HSV color space because it is independent of light intensity.

Given equation 4, we can call $\bar{y}(\bar{y}_R, \bar{y}_G, \bar{y}_B)$ one color of the object perceived at an unknown distance and at a particular lighting value. We can take this color from any picture of the object. We will use this prior color as a reference, and we will assume for it $d = 0$ and $\ell = 1$. It should be noted that if this color comes from a picture of the object taken at 3 meters, its color at a shorter distance will cause a negative value in the equation (X-axis on the Fig.2). Finally, we need an estimation of the attenuation coefficient $C(c_R, c_G, c_B)$. These coefficients can be estimated using different methods. In Section IV-B, details will be given about the method we use that only requires few pictures of the object at different distances.

Therefore, we can define the function f which can give all the compatible colors of \bar{y} depending on ℓ and d (see Fig. 2):

$$f : \begin{cases} \mathbb{R}^2 \rightarrow \mathbb{R}^3 \\ (d, \ell) \mapsto \begin{cases} y_R = \ell \cdot \bar{y}_R \cdot e^{-c_R \cdot d} \\ y_G = \ell \cdot \bar{y}_G \cdot e^{-c_G \cdot d} \\ y_B = \ell \cdot \bar{y}_B \cdot e^{-c_B \cdot d} \end{cases} \end{cases} \quad (5)$$

The set of colors generated by this function is illustrated on the diagram in Fig. 2. It shows the modification of the color along two axes: distance d (X-axis) and light ℓ (Y-axis). The prior known color we are looking for is inside the small white circle of coordinate (0,1). The black area represents out-of-bound colors. The figure shows that negative distance appears. Indeed, we consider the case where the prior has been chosen

on a picture of an object taken underwater. It is sometimes impossible to get a picture of an object outside the underwater media.

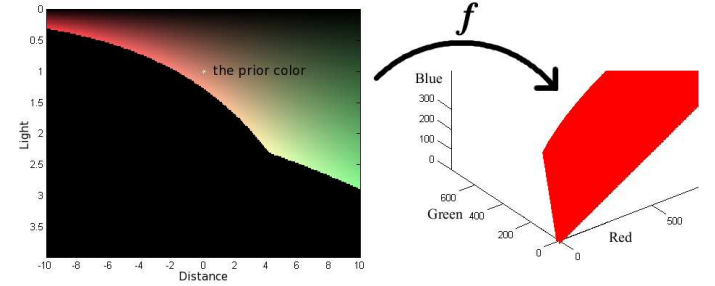


Fig. 2. Illustration of the compatible color surface. The f function associates a distance d and a lighting ℓ with a color. The set of compatible colors for \bar{y} (200, 130, 110) and $c_R = 0.142$, $c_G = 0.039$, $c_B = 0.076$ is shown applying the parameters $d \in [-10, 10]$, $\ell \in [0, 4]$.

Two colors y and \bar{y} are compatible if:

$$\exists(d, \ell), y = f_{C, \bar{y}}(d, \ell), \quad (6)$$

IV. ALGORITHM FOR COLORED OBJECT RECOGNITION

A. Context of use

It has to be noted that backscatter of a light source is not considered. From a practical point of view it may be neglected in many cases. Unfortunately if we consider dark colors it is going to produce a bias in the physically compatible colors with regards to the estimated ones. It results in poorer recognition performances. Since this component is difficult to take into account and because the dark colors are compatible with any prior color, we have restricted our study to bright colors. The generalization of our method taking into account the backscattering component will be studied in a future work.

B. The estimation of the attenuation parameters

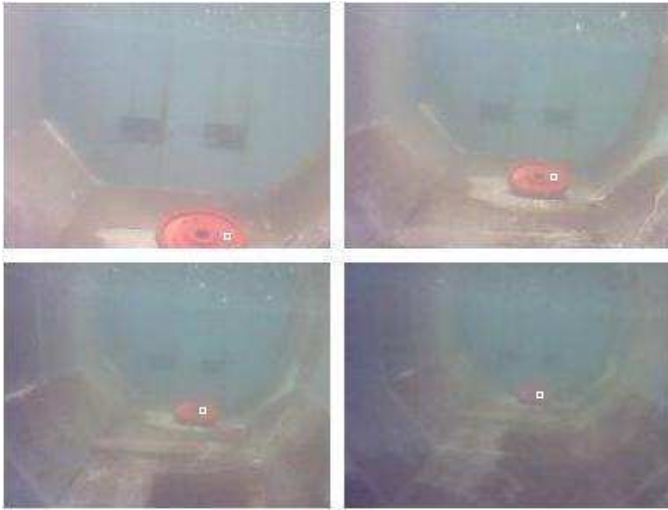
As stated previously, many methods exist to compute the attenuation parameters, but they usually require additional equipment and a complicated calibration procedure [3][13]. In our case, a simpler method is used, it is less accurate but easy to carry out and sufficient for our purpose. Our method only requires a few pictures of an object at different distances to estimate roughly the attenuation coefficients of the underwater environment. In real applications, we normally have the possibility to do some remote controlled runs, navigating towards an object and taking some pictures before the actual autonomous run.

This method is fully described in our previous article [1] but can be summarized by the following points:

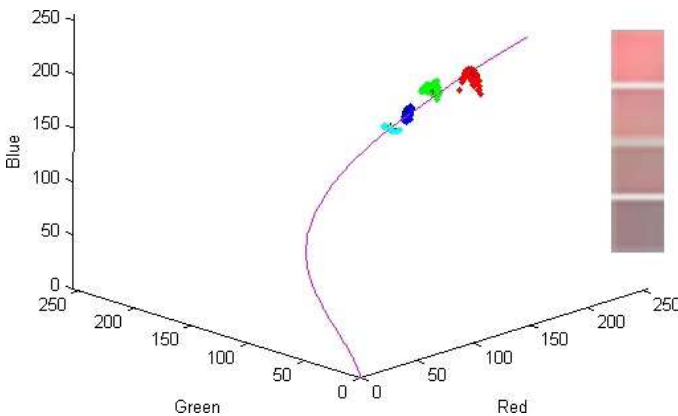
- 1) sub images extraction from the images corresponding to the object at different distances (Fig. 3.a).
- 2) sub images processing by Gaussian filtering.
- 3) extraction of a collection of RGB triplet corresponding to the color of the object at several distances.

- 4) normalization of RGB values. Red, green, and blue pixel values are divided by the sum of RGB pixel values,
- 5) least square estimation of the attenuation curve based on the normalized RGB values extracted from the sub images (Fig. 3.b).

In order to improve the results we recommend to repeat the coefficients estimation few times with different sub images and to take the median values of the estimations. We will show in the next part that in order to use equation 8 effectively the three coefficients must differ from each other. The probability of obtaining identical attenuation coefficients is very low, unfortunately if this particular case occurs at all, the process must be repeated. From a practical point of view, this inaccuracy can be due to the noise in the image data, to the choice of the colored sub images, to the Gaussian filter and to the numerical approximation.



(a)



(b)

Fig. 3. (a) Underwater images of a red disk (248, 149, 144) at 2, 3, 4, 5 meters used for calibration. (b) Estimation of the attenuation coefficients using four sub images (whites squares) extracted from pictures of a red disk at different distances. The four point clouds used here to estimate the medium coefficients refer to the four white squares.

C. Detection of the compatible colors

Given the assumed model (Eq. 3), we studied a situation in an underwater environment:

- 1) First, we consider a white light source of intensity q_a . This source illuminates an object whose absorption coefficients are (a_R, a_G, a_B) . A camera observes this object and the perceived color is called $y(y_R, y_G, y_B)$. Let l_a be the distance traveled by the light from the source to the camera.
- 2) Secondly, the intensity of the light source and the object's position change. Let q_b be the new intensity, l_b the new distance and $z(z_R, z_G, z_B)$ the new color received by the camera.

The vector $C(c_R, c_G, c_B)$ stands for the attenuation coefficients of the three wavelengths (red, green, blue) supposed known, and $y_R, y_G, y_B, z_R, z_G, z_B, q_a, q_b$ are supposed strictly positive (two particular cases are not considered, the true black object and the zero lighting case). The colors $y(y_R, y_G, y_B)$ and $z(z_R, z_G, z_B)$ received by the camera come from the same object, they are compatible from an underwater point of view. We have:

$$\begin{cases} y_R = q_a \cdot a_R \cdot e^{-c_R \cdot l_a}, \\ y_G = q_a \cdot a_G \cdot e^{-c_G \cdot l_a}, \\ y_B = q_a \cdot a_B \cdot e^{-c_B \cdot l_a}, \\ z_R = q_b \cdot a_R \cdot e^{-c_R \cdot l_b}, \\ z_G = q_b \cdot a_G \cdot e^{-c_G \cdot l_b}, \\ z_B = q_b \cdot a_B \cdot e^{-c_B \cdot l_b}. \end{cases}$$

By removing variables (a_R, a_G, a_B) , we get:

$$\begin{cases} \frac{y_R}{z_R} = \frac{q_a}{q_b} \cdot e^{c_R \cdot (l_b - l_a)}, \\ \frac{y_G}{z_G} = \frac{q_a}{q_b} \cdot e^{c_G \cdot (l_b - l_a)}, \\ \frac{y_B}{z_B} = \frac{q_a}{q_b} \cdot e^{c_B \cdot (l_b - l_a)}. \end{cases}$$

In the same way we can remove the intensity ratio $\frac{q_a}{q_b}$, then we have:

$$\begin{cases} \frac{y_R \cdot z_G}{z_R \cdot y_G} = e^{(c_R - c_G) \cdot (l_b - l_a)}, \\ \frac{y_R \cdot z_B}{z_R \cdot y_B} = e^{(c_R - c_B) \cdot (l_b - l_a)}. \end{cases}$$

Or equivalently,

$$\begin{cases} \log\left(\frac{y_R \cdot z_G}{z_R \cdot y_G}\right) = (c_R - c_G) \cdot (l_b - l_a), \\ \log\left(\frac{y_R \cdot z_B}{z_R \cdot y_B}\right) = (c_R - c_B) \cdot (l_b - l_a). \end{cases}$$

Finally, we remove $(l_b - l_a)$,

$$(c_R - c_B) \cdot \log\left(\frac{y_R \cdot z_G}{z_R \cdot y_G}\right) - (c_R - c_G) \cdot \log\left(\frac{y_R \cdot z_B}{z_R \cdot y_B}\right) = 0.$$

If we note $C = \left(\frac{c_R - c_G}{c_R - c_B}\right)$ we get:

$$(1 - C) \cdot \log(y_R) - \log(y_G) + C \cdot \log(y_B) = (1 - C) \cdot \log(z_R) - \log(z_G) + C \cdot \log(z_B). \quad (7)$$

This last equation leads to:

Two colors y and \bar{y} are compatible if:

$$\psi(y, \bar{y}) \in [C - \epsilon, C + \epsilon]. \quad (8)$$

$$\text{with } \psi(y, \bar{y}) = \frac{\log(y_G) - \log(\bar{y}_G) - \log(y_R) + \log(\bar{y}_R)}{\log(y_R) - \log(\bar{y}_R) - \log(y_B) + \log(\bar{y}_B)}.$$

$$\text{and } C = \frac{c_R - c_G}{c_R - c_B} \text{ with } c_R \neq c_B.$$

Eq. 8 is the color compatibility condition. In other words, by using the prior knowledge of a color we are able to detect all its compatible colors in an underwater environment, that is to say colors perceived at different distances and at different lighting intensities. Thus, by applying this function to each pixel and by assigning it to the compatible color class or not we obtain a binarization of the image. Therefore, depending on the number of compatible colors, we decide if the object we are looking for is in the image or not.

If necessary we can also post process the segmented image using a mathematical morphology algorithm to improve the binary image by gathering pixels in a concentrated area and by suppressing isolated pixels (false alarms). It should be noted that the recognition results presented in the next section are the raw result obtained without any post processing.

D. Improve robustness by adding constraints on the compatible color surface

To reduce the number of compatible colors we added some constraints. These constraints aim to make the algorithms more robust and to decrease the false alarms rate (see Fig. 4). The first constraint is an upper limit of the distance. It considerably limits the false alarms by suppressing the colors situated too far from the prior known color. Its value depends on underwater visibility. It can be easily estimated as we have previously computed the attenuation parameters. For example, only considering the red component of the prior color which is usually the greater, we assign this constraint to the distance required to loose 90% of the initial value of the red component. Using Eq. 2 with \bar{y} (200, 130, 110) for $c_R = 0.241$, we obtain the distance: 9,36m.

Secondly, we add a constraint on the light parameter to disregard the dark colors which are compatible with any other colors. Since our previous detection method [1], we have replaced the empirical threshold by thresholds with a real physical meaning.

To sum up, two colors y and \bar{y} are compatible, that is to say they correspond to the same color modified by the underwater medium if:

- It belongs to the surface: $\psi(\bar{y}, y) \in [C_{min}, C_{max}]$.
- It respects the distance constraint:

$$d_{min} < \frac{1}{c_G - c_R} \cdot \log\left(\frac{y_R \cdot \bar{y}_G}{\bar{y}_R \cdot y_G}\right) < d_{max}$$

- It respects the light constraint:

$$\left(\frac{y_R}{\bar{y}_R}\right) \cdot \left(\frac{y_R \cdot \bar{y}_G}{\bar{y}_R \cdot y_G}\right)^{\frac{c_R}{c_G - c_R}} > l_{min}$$

$$\text{with } c_G \neq c_R \text{ and } \bar{y}_R \neq y_G \neq 0$$

V. EXPERIMENTAL RESULTS

Fig. 5.a shows real underwater images of a red disk in a tank filled of water and the compatible colors detected considering the whole set of compatible colors. Fig. 5.b shows the segmentation considering the constrained set of compatible colors.

To give a better idea, we have tested a color segmentation using the HSV (Hue, Saturation, Value) space which is known

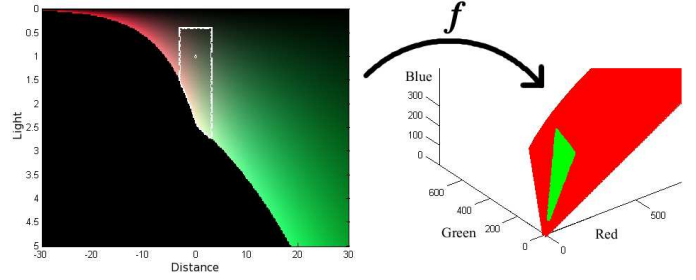


Fig. 4. Set of compatible colors with the prior color (110, 106, 88) obtained by applying constraints on distance and light. The prior color is in the small white circle and the compatible colors are enclosed by a white polygon ($d_{min} = d_{max} = 3$ meters, and $l_{min} = 0.5$).

TABLE I
QUANTITATIVE RESULTS ON DIFFERENT SEQUENCES.

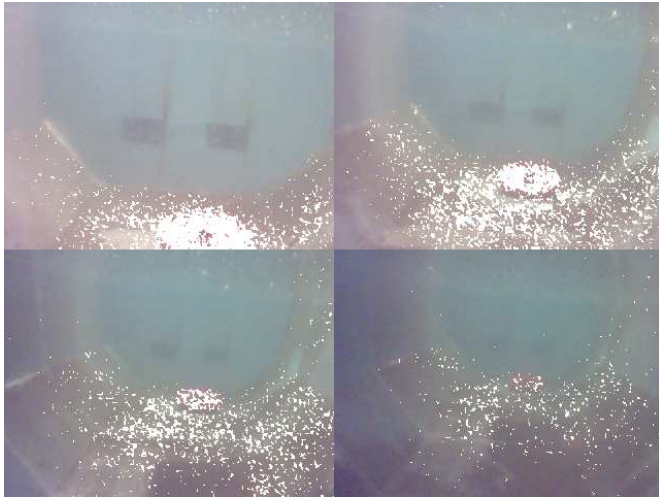
Tank	Ground Truth	False alarms	Missed pixels
ENSTA Br. (Fig. 5.a)	11600	18%	7%
ENSTA Br. (Fig. 5.b)	11600	1%	5%
ENSTA Br. (Fig. 5.c)	94800	5%	4%
ENSTA Br. (Fig. 6)	11600	38%	5%
GESMA (Fig. 8.a)	14520	0%	35%
IFREMER (Fig. 8.b)	3420	0%	40%
IFREMER (Fig. 7.a)	1156	0%	65%
IFREMER (Fig. 7.b)	1156	0%	69%
IFREMER (Fig. 7.c)	7806	0%	45%
IFREMER (Fig. 7.d)	7806	0%	52%

as a robust space for color segmentation [11][12][25]. The hue of the object is computed from the RGB values and we assign each pixel to the object class or not, according to the proximity to the hue. To keep an objective point of view we have applied the threshold to obtain the same detection rate (Fig. 6), that is to say nearly the same number of pixels detected on the object by each of the two methods. We can clearly see comparing the results that the false alarms rate is really more important in hue space although we have the same false negative rate. By comparing Fig. 5.b and 6, we can see that our recognition method leads to fewer false alarms and a better detection rate than the method of reference does. For example, in the hue space it is more difficult to distinguish the object from the bottom of the tank.

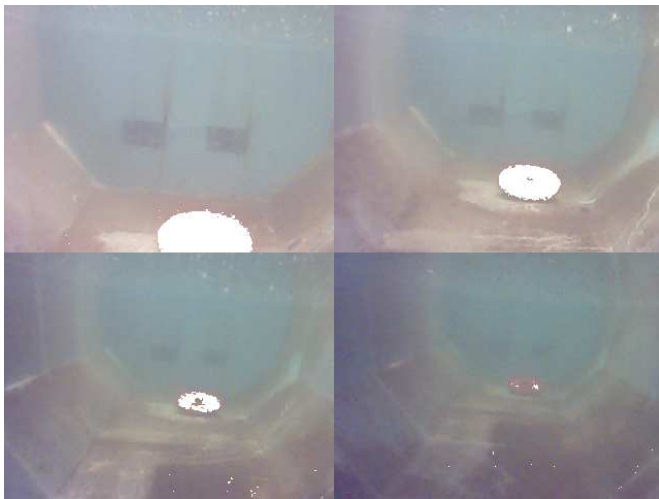
The addition of the constraints considerably improves the results. We can notice on Fig. 5.c that the glint of the object on the water surface is also well detected as a compatible color

TABLE II
ENVIRONMENTAL INFORMATION ON THE PRESENTED SEQUENCES.

	Experiments details
ENSTA Br. (Fig. 5.a)	Clear water, 1 red disk, low threshold.
ENSTA Br. (Fig. 5.b)	Clear water, 1 red disk, low threshold.
ENSTA Br. (Fig. 5.c)	Clear water, 1 red disk, low threshold.
ENSTA Br. (Fig. 6)	Clear water, 1 red disk, low threshold.
GESMA (Fig. 8.a)	Turbid salty water, 1 orange ball.
IFREMER (Fig. 8.b)	Salty water, 2 yellow traffic cones.
IFREMER (Fig. 7.a)	Salty water, 2 yellow traffic cones.
IFREMER (Fig. 7.b)	Salty water, 2 yellow traffic cones, 1 orange ball.
IFREMER (Fig. 7.c)	Salty water, 2 yellow traffic cones, 1 orange ball.



(a)



(b)



(c)

Fig. 5. Segmentation results on a set of images taken at ENSTA-Bretagne in tank filled of clear water. (a) Compatible colors without applying constraints. (b) Compatible colors by applying constraints on distance and light. (c) Compatible colors with the same prior color obtained by applying constraints under different conditions (different distances, different lighting intensities and another object position). The two last images were taken in the evening when the light is limited.

(see last image). The proposed approach has also been tested on real data in real underwater contexts. It has been used for two years at SAUC’E competition (IFREMER images), in the

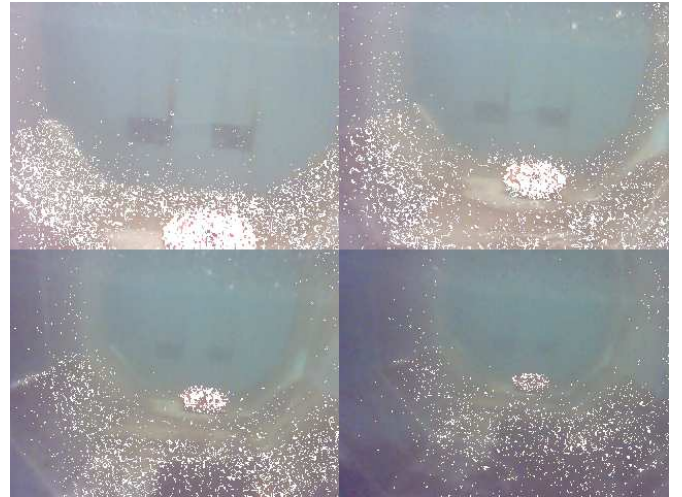


Fig. 6. Compatible colors in the hue space with the RGB color (248, 149, 144).

recognition and tracking of a colored target object we need to intercept. Different examples obtained during real robot run are presented on Fig. 7, 8. In order to show the robustness of our method we have selected results in various underwater media, different lighting conditions and using different colored objects at different distances. Table II gives some information about the different media and objects we were looking for. Table I gives some qualitative results. The first column gives the number of pixels corresponding to the target object while the second and the third give the false positive and false negative rate. Those results show the algorithm used with drastic constraints recognizes about 50% of the compatible pixels without any false alarm. It must be noted that the first lines of the table showing higher false alarm rates also show very low false positives rate. The constraints have been selected to reduce as much as possible the false positives rate. With regards to the other results, they were obtained during real robotic contest, so the constraints have been settled to reduce the false alarm rate. Practically, a detection rate around 50% is sufficient to recognize an object and localize it in an image. Focusing on bright colors since dark ones are difficult to detect, we have shown that the method works well with colors similar to the background (bottom of the tank, see Fig. 5). Furthermore, simultaneous detections of multiple targets has been demonstrated on Fig. 7.c and Fig. 7.d. For this work, the only requirement is that the target colors must be on different compatible surfaces to be distinguishable from each other.

VI. CONCLUSIONS AND FUTURE WORK

In many robotic applications it is necessary to identify a known object by using a vision system. An object can generally be characterized by its shape, its color, sometimes its size or its texture. In an underwater environment (contrary to a terrestrial one), it is difficult to recognize an object by observing its color because of light attenuation. The shape is often favored. However, when we are looking for known objects the color remains a simple and robust feature [1].

In this article, we propose a new object recognition technique based exclusively on the color feature. The proposed method consists of detecting colors compatible with the color of a given object by taking into account the underwater color constancy problem. This color-based method is naturally robust to partial occlusion, object position and scale change. The implemented algorithm works directly on the raw data, it is fast and needs few computers resources. It is really convenient for robotic applications where computer resources are limited and shared between different robot components. The compatible color concept considering light attenuation in water leads to a new color-based recognition method. It enables the use of color in many underwater robot applications such as target interception, object tracking or obstacle detection. The proposed method has also to be assessed on more images in different conditions to be definitively validated.

As such, we successfully used our approach when experimenting for SAUC'E competition (Student Autonomous Underwater Challenge - Europe⁵). The method only considers bright colors, because dark colors are compatible with any color and we do not take into account the backscattered component in our model. The possibility to process dark colors is a further topic of research. Results are promising and can be improved by taking into account the temporal feature. Consequently our future work will be to improve robustness by varying the constraints over the time. This local refinement could consist for example in strengthening the constraints to avoid false alarms when there are no compatible colors, but to relax it in the neighborhood of a compatible pixel when compatible colors begin to be detected.

REFERENCES

- [1] , "_____, ____," in _____.
- [2] J. Ahlen, "Color correction of underwater images using spectral data," Ph.D. dissertation, Uppsala University, Centre for Image Analysis, 2005.
- [3] J. Ahlen, E. Bengtsson, and T. Lindell, "Color correction of underwater images based on estimation of diffuse attenuation coefficients," in *Proc. of PICS conference*, 2003.
- [4] M. Chambah, D. Semani, A. Renouf, P. Courtellemont, and A. Rizzi, "Underwater color constancy: enhancement of automatic live fish recognition," in *Proceedings of SPIE*, vol. 5293, 2003, pp. 157–168.
- [5] G. Dudek *et al.*, "A visually guided swimming robot," in *Proc. IEEE International Conference on Intelligent Robots and Systems*, 2005, pp. 3604–3609.
- [6] S. Q. Duntley, *Light in the sea*. J. Opt. Soc. Am., 1963.
- [7] G. L. Foresti and S. Gentili, "A vision based system for object detection in underwater image," in *Proc. IEEE International Conference on Computer Vision and Pattern Recognition*, vol. 14, 2000, pp. 544–549.
- [8] T. Gevers and A. W. M. Smeulders, "Color based object recognition," *Pattern Recognition*, vol. 32, pp. 453–464, 1999.
- [9] H. R. Gordon, "Can the lambert-beer law be applied to the diffuse attenuation coefficient of ocean water," *Limnology and Oceanography*, vol. 34, 1989.
- [10] N. G. Jerlov, *Marine optics*. Elsevier oceanography series, 1976.
- [11] G. J. Klinker, S. A. Shafer, and T. Kanade, "A physical approach to color image understanding," *International Journal of Computer Vision*, vol. 4, pp. 7–38, 1990.
- [12] V. Kravtchenko, "Tracking color objects in real time," Ph.D. dissertation, University of British Columbia, 1999.
- [13] D. R. Mishra, S. Narumalani, D. Rundquist, and M. Lawson, "Characterizing the vertical diffuse attenuation coefficient for downwelling irradiance in coastal waters," *ISPRS Journal of photogrammetry and remote sensing*, vol. 60, pp. 48–64, 2005.
- [14] S. Obdrzalek, J. Matas, and O. Chum, "On the interaction between object recognition and colour constancy," in *Proc. IEEE International Conference on Computer Vision (ICCV03)*, 2003.
- [15] A. T. Olmos-Antillon, "Detecting underwater man-made objects in unconstrained video image," Ph.D. dissertation, Heriot Watt University, Department of Computing and Electrical Engineering, 2002.
- [16] Y. Petillot, I. T. Ruiz, and D. M. Lane, "Underwater vehicle obstacle avoidance and path planning using a multi-beam forward looking sonar," *IEEE Journal of Oceanic Engineering*, vol. 26, pp. 240–251, 2001.
- [17] G. L. Pickard and W. J. Emery, *Descriptive Physical Oceanography: An Introduction, 5th enlarged ed.* Oxford: Pergamon Press., 1990.
- [18] O. Pizarro and H. Singh, "Toward large-area mosaicing for underwater scientific applications," *Robotics: Science and Systems VI*, vol. 28, pp. 651–672, 2003.
- [19] S. Reed, Y. Petillot, and J. Bell, "An automatic approach to the detection and extraction of mine features in sidescan sonar," *IEEE Journal of Oceanic Engineering*, vol. 28, pp. 90–105, 2003.
- [20] J. Sattar, P. Giguere, G. Dudek, and C. Prahacs, "A visual servoing system for an aquatic swimming robot," in *Proc. IEEE International Conference on Intelligent Robots and Systems*, 2005, pp. 1483–1488.
- [21] Y. Y. Schechner and N. Karpel, "Clear underwater vision," in *Proc. IEEE International Conference on Computer Vision and Pattern Recognition*, vol. 1, 2004, pp. 536–543.
- [22] D. Semani, M. Chambah, and P. Courtellemont, "Processing of underwater color images applied to live aquarium videos," *Int. Journal of Robotics and Automation (IJRA)*, vol. 20, pp. 123–130, 2005.
- [23] S. Skaff and al., "Estimating surface reflectance spectra for underwater color vision," in *Proc. of the British Machine Vision Conference, Leeds, U.K.*, vol. 2, 2008, pp. 1015–1024.
- [24] R. H. Stavn, "Lambert-beer law in ocean waters: optical properties of water and of dissolved/suspended material, optical energy budgets," *Applied Optics*, vol. 27, pp. 222–231, 1988.
- [25] S. Sural, G. Qian, and S. Pramanik, "Segmentation and histogram generation using the hsv color space for image retrieval," in *Proc. IEEE International Conference on Image Processing*, vol. 2, 2002, pp. 589–592.
- [26] I. Vasilescu, C. Detweiler, and D. Rus, "Color-accurate underwater imaging using perceptual adaptive illumination," in *Robotics: Science and Systems VI (RSS2010)*, 2010.
- [27] D. Walther, D. R. Edgington, and C. Koch, "Detection and tracking of objects in underwater video," *IEEE Computer Vision and Pattern Recognition*, vol. 1, pp. 544–549, 2004.
- [28] A. Yamashita, M. Fujii, and T. Kaneko, "Color registration of underwater of images for underwater sensing with consideration of light attenuation," in *Proc. IEEE International Conference on Robotics and Automation*, Roma, 2007, pp. 4570–4575.
- [29] P. Zingaretti and S. M. Zanoli, "Robust real-time detection of an underwater pipeline," *Engineering Applications of Artificial Intelligence*, vol. 11, pp. 257–268, 1998.

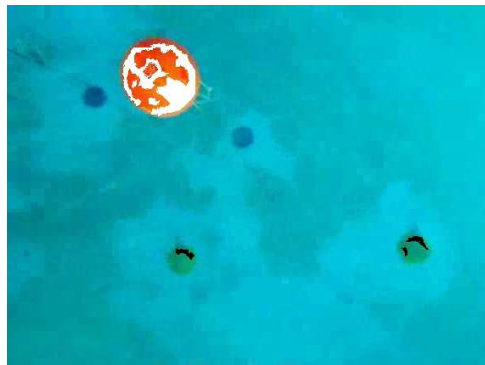
⁵http://www.dstl.gov.uk/news_events/competitions/sauce/index.php.



(a)



(b)

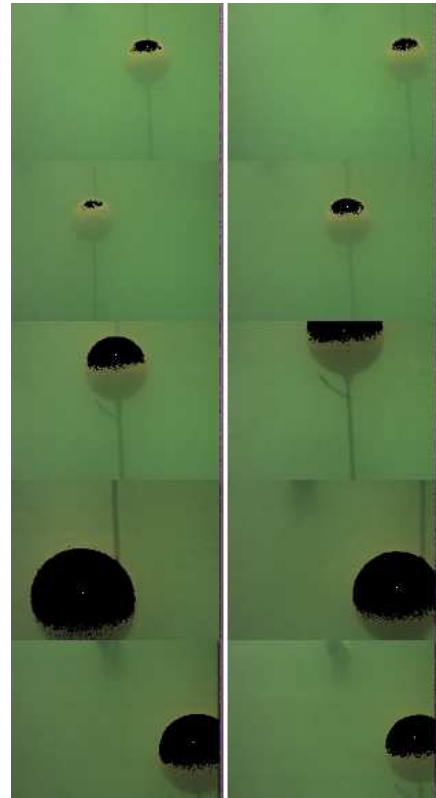


(c)

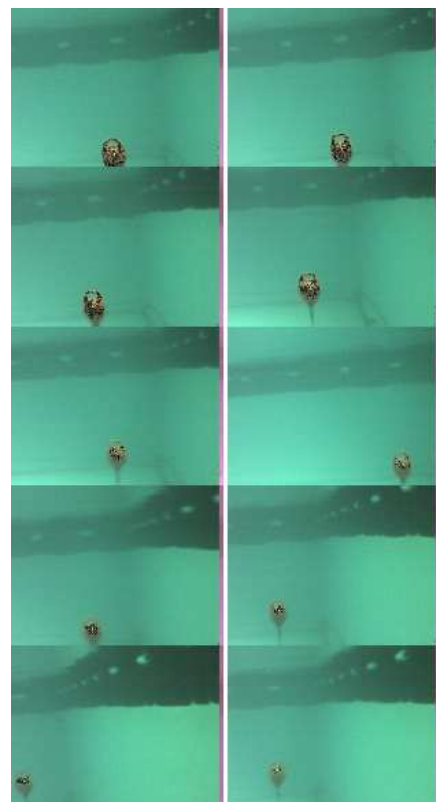


(d)

Fig. 7. Set of images taken at IFREMER in a 10 meters depth pool (a)(b) Black pixels are the compatible colors with the two yellow traffic cones obtained by applying constraints. (c)(d) Black and white pixels are the compatible colors with two different objects: an orange ball and two yellow traffic cones under different lighting conditions.



(a)



(b)

Fig. 8. (a) Recognition results on two others sequences (a) Set of images at GESMA in a very turbid water at short range. (b) Set of images at IFREMER in salty water at large range. The threshold is lower in the second sequence because visual aliasing was important. Those images highlight the decrease of the visibility with distance.